Annals of Nuclear Energy 202 (2024) 110463

Contents lists available at ScienceDirect

Annals of Nuclear Energy

journal homepage: www.elsevier.com/locate/anucene

A reactivity meter with uncertainties

Adimir dos Santos

Instituto de Pesquisas Energéticas e Nucleares – IPEN/CNEN-SP, Centro de Engenharia Nuclear (CEN), Av. Prof. Lineu Prestes, 2242, 05508-000 - Cidade Universitária, São Paulo, SP, Brazil

ARTICLE INFO

Keywords:
Reactivity uncertainty
Inverse kinetic model
Kinetics parameter uncertainties
Reactivity meter with uncertainty
Spectral densities

ABSTRACT

Three sets of effective kinetics parameters were measured and evaluated for the fuel rod core of the IPEN/MB-01 research reactor. A correlation matrix among all these effective kinetics parameters is taking into account to reduce the inferred reactivity uncertainties. This work considers the propagation of the uncertainties inherent in these sets of effective delayed neutron parameters to the inferred reactivities. The comparisons to the reactivity and its uncertainty values produced by the Inhour Equation came into a very good agreement and reinforces the validity of the whole procedure for the development of this reactivity meter with uncertainties. The reduction of the reactivity uncertainty values compared to previous works is significant. The analyses of some specific cases of the evaluation IPEN(MB01)-LWR-RESR-015 reveal that its reactivity values are in accordance with those of this work. However, its reactivity uncertainty values for positive reactivities seems to cancel the uncorrelated component of the uncertainties.

1. Introduction

Reactivity is an integral reactor response and plays an important role in the nuclear engineering field. It has important bearings on the reactor design, on its operational and safety performance and on the fuel cycle strategy. The importance of its measurements has been recognized since the first experimental atomic pile in Chicago, which took place on December 2, 1942 (Fermi, 1946). Since then, the measurements of this very important integral reactor response have been addressed by several works such as: (Henry, 1958); in the fifties, (Andersson and Hveding, 1964) in the sixties and more recently by (Marie et al., 2019), (Huo et al., 2019), and (Vo et al., 2023).

Reactivity is not a quantity that is directly measured. Instead, it is inferred from the detector signals in conjunction with a set of effective kinetics parameters and a kinetic model. By kinetics parameters are meant the whole set of delayed neutron parameters plus the prompt neutron generation time. There are two major categories of reactivity measurements: a) Reactivity measurements close to the critical state which are encompassed by the Inverse Kinetic Method (IKM) (Sastre, 1960) and by the Doubling Time Method or PM – Period Method (DTM) (Hassan et al., 2010) and b) the Subcritical Measurements which are encompassed by the Source Multiplication Method (MSM) (Blaise et al., 2009) and (Krása et al., 2021), the neutron noise method (Momura,1966) among several others. This paper concerns the methods of reactivity measurement closed to the critical state and more specifically the IKM model.

The IKM can be considered a dynamic reactivity method (Ott and Neuhold, 1985) and at the same time an on-line method. The IKM method infers the reactivity sequentially as a function of time. The starting point for the IKM method was due to Sastre in 1960 (Sastre, 1960). The main assumptions for Sastrés IKM was the validity of the point kinetics model (Bell and Glasstone, 1979) as they are known nowadays and the validity of calculated effective kinetics parameters. Later, the IKM method was subject to several works and improvements as described in (Andersson and Hveding, 1964), (Suzuki and Tsunoda, 1964) and in (Ott and Neuhold, 1985). Most of the applications addressed thermal rectors (Kinard and Allen, 2004), (Ball, 2017), (Lee et al.,2005), among several others. However, a few applications addressed ADS (Muñoz-Cobo et al., 2001) and subcritical systems driving by a neutron source (Tamura, 2003). More recent works can be found in (Dulla et al.,2017), (Huo et al., 2019), and (Vo et al., 2023). The IKM method has been extremely benefited from the progress reached in the computer technology as well as in the signal acquisition systems which allow it to monitor the reactivity in a nuclear reactor practically in real time (Dulla et al., 2014).

The effective delayed neutron parameters are the main input data and the major source of uncertainties for the IKM methodology. They are reactor dependent data because they are weighted by the adjoint and direct neutron fluxes of the reactor under analyses (Bell and Glasstone, 1979). The delayed neutrons in a nuclear reactor arise from the

E-mail address: adsantos@alumni.usp.br.

https://doi.org/10.1016/j.anucene.2024.110463
Received 18 October 2023; Received in revised form 24 February 2024; Accepted 2 March 2024
Available online 14 March 2024

radioactive decay of specific classes of fission products. These fission products are referred to as the delayed neutron precursors. An experimental characterization of all these emitters is very difficult due to their low yield and/or low half-lives and also due to their very complex transmutation chains. The point kinetics equations employed by the IKM methodology needs only the aggregate behavior of the delayed neutrons consisting of a few-group model where the decay constants and abundances are mean values of various precursor emitters with similar decay constants. A six-group model first introduced by Keepin (Keepin et al., 1957) was considered a standard for many years. Some recent work considers an eight-group delayed neutron model based on a consistent set of half-lives (Spriggs et al., 2002).

The major source of delayed neutron nuclear data is the ENDF (Evaluated Nuclear Data File) file (Trkov et al., 2018). Examples of such files are ENDF/B-VIII.0 (Brown, 2018) and JENDL 4.0 (Shibata et al., 2011). The NJOY system (MacFarlane et al., 2017) is a set of computer module that process the ENDF files and builds the nuclear data libraries (multigroup or pointwise) for several applications including those related to the delayed neutron applications. Most of the delayed neutron evaluations contained in ENDF files relies either on calculation methods such as those employed in CINDER-90 (Wilson and England, 2002) and in (Brady and England, 1989) or on the out-of-pile experiments (Spriggs and Campbell, 2000). These experiments consider the irradiation of a specific actinide sample in the reactor core and by means of a fast removal system this sample is removed and transferred to the out-of-core neutron detector system. The measured data (basically neutron detector counts) as a function of time are least squares fitted in a series of exponentials terms and the delayed neutron abundances and their respective decay constants are inferred from them. Both the calculated and experimental approaches may consider the total delayed neutron fraction normalization from other experiments.

The available experimental support to validate methods and nuclear data for the determination of the effective kinetics parameters and consequently the reactivity is scarce and in many cases of very difficult utilization. The lack of specific benchmarks to verify the quality of the reactivity determination is a severe problem in the reactor physics area (dos Santos and Diniz, 2014). Aiming to contribute to this specific need for thermal reactor application a wide variety of experiments addressing the effective kinetics parameters were performed at the IPEN/MB-01 research reactor facility. Most of them are available in the IRPhE (International Reactor Physics Experiments) handbook as IPEN(MB01) contributions. The experiments ranged from the measurements of the prompt neutron generation time (Λ) (Diniz and dos Santos, 2006), (Kuramoto et al., 2007), (Kuramoto et al., 2008) and (dos Santos et al., 2006a), its lifetime in the core (τ_c) and in the reflector (τ_r) (Santos and dos Santos, 2021), to the effective delayed neutron data as: the effective delayed neutron fraction (β_{eff}) (Diniz and dos Santos, 2006), (Kuramoto et al., 2007), (Kuramoto et al., 2008), the first decay constant (λ_1) (dos Santos et al., 2006b), and the delayed neutron abundances (β_i/β_{eff}) and their decay constant (λ_i) (Diniz and dos Santos, 2006) for group i in a six-group model. The results of these experiments were all gather to build a set of six-group kinetic parameters for the IPEN/MB-01 reactor. The details of this process are extensively described in IPEN(MB01)-LWR-RESR-021 (dos Santos, 2021). This evaluation was approved by the IRPhE and it is available in its website. Finally, a correlation matrix for the effective delayed neutron fraction (β_i) and their decay constant (λ_i) (dos Santos and Diniz, 2020) was also developed aiming to reduce the inferred reactivity uncertainties.

The reported IKM applications share some common characteristics such as the validity of point kinetics equations, the utilization of calculated effective kinetics parameters, and neither of them addressed a very important subject: propagation of the uncertainties of the effective kinetics parameters to the inferred reactivities. The purposes of the present work are to develop a method to propagate the uncertainties arising from the effective kinetics parameters in a six-group model to the reactivities inferred by the IPEN/MB-01 inverse kinetic model algorithm. The effective kinetics parameters as well as their uncertainties arise from the IPEN(MB01)-LWR-RESR-021 evaluation. The accuracy of this development will be verified against the results arising from the application of the Inhour equation model. Furthermore, the procedures developed in this paper to treat the reactivity uncertainties will be employed to verify the adequacy of the reactivity and its uncertainty models employed in IPEN(MB01)-LWR-RESR-015 (dos Santos et al., 2014).

2. The methodology for the reactivity meter with uncertainties

The proposed methodology to propagate the uncertainties inherent in the effective kinetics parameters to the reactivity is based on the IKM (Inverse Kinetics Method) methodology. Here, the point kinetics equation is taken into account for the dynamic behavior of the reactor system and the reactivity is written as an explicit function of time and an implicit function of effective kinetics parameters and the neutron detector signals. Next, a standard uncertainty analysis for the propagation of the uncertainties of the effective kinetics parameters to the reactivity values is employed and the reactivity uncertainty analysis can be performed accordingly.

2.1. The IPEN/MB-01 inverse kinetic method (IKM) for reactivity measurements

The inverse kinetic method implemented in the IPEN/MB-01 reactivity meter starts with the point kinetics equations in a six-group delayed neutron model as:

$$\frac{dN(t)}{dt} = \frac{\rho(t) - \beta_{eff}}{\Lambda} N(t) + \sum_{i=1}^{6} \lambda_i C_i(t), \tag{1}$$

and

$$\frac{dC_i(t)}{dt} = \frac{\beta_i}{\Lambda} N(t) - \lambda_i C_i(t), \tag{2}$$

where:

$N(t)$ represents the detector signal (ampere) at time t,

$\rho(t)$ represents the reactivity at time t,

β_i represents the effective delayed neutron fraction for delayed neutron group i,

β_{eff} represents the total effective delayed neutron fraction,

λ_i represents the decay constants for the delayed neutron group i,

$C_i(t)$ represents the precursor concentration of the ith delayed neutron group at time t,

and Λ represents the prompt neutron generation time.

The point kinetics equations represented by Eqs. (1) and (2) are a system of coupled linear ordinary differential equations. The time-dependent parameters in this system of equations are the reactivity ($\rho(t)$), the detector signal ($N(t)$), and the concentration of the ith delayed neutron precursor ($C_i(t)$). All the effective kinetics parameters and the detector signal ($N(t)$) in this system of equations are assumed to be known. Consequently, the only unknown in this set of equations is the reactivity ($\rho(t)$). The basic principle for the IKM methodology considers this system of equations and solves that for the reactivity ($\rho(t)$) in the following steps. Initially Eq. (2) is solved for $C_i(t)$ and the final result is placed into Eq. (1). Next, the resulting equation is solved for the reactivity ($\rho(t)$) and the following equation is found:

$$\rho(t) = \frac{\Lambda}{N(t)} \frac{dN(t)}{dt} + \beta_{eff} - \frac{\Lambda}{N(t)} \sum_{i=1}^{6} \lambda_i C_i(0) e^{-\lambda_i t} - \frac{1}{N(t)} \sum_{i=1}^{6} \lambda_i \beta_i e^{-\lambda_i t} \int_0^t N(t\hat{A}) e^{\lambda_i t\hat{A}} dt\hat{A}. \tag{3}$$

The initial conditions for $C_i(0)$ is found assuming that the reactor is critical at $t = 0$ as:

$$C_i(0) = \frac{\beta_i}{\lambda_i \Lambda} N(0), \tag{4}$$

where $N(0)$ is the initial value of the detector signal and it is obtained when the reactor is critical, just before the insertion of reactivity. Eqs. (3) and (4) constitute the starting point for the IKM methodology. The software designed to solve Eq. (3) is referred to as the reactivity meter and it is widely employed in research and power reactors.

The approach adopted in the reactivity meter developed in the IPEN/MB-01 research reactor facility considers that the detector signals are given in a set of discrete time intervals $(t_1, t_2, \cdots, t_k, t_{k+1}, \cdots, t_M)$. Here t_k and t_{k+1} are two generic and consecutive time intervals and M is total number of time intervals. Next, Eq. (3) is written in a recursive, simplified, and compact form for a generic time t_{k+1} as:

$$\rho_{k+1} = X_{k+1} - \frac{\Lambda}{n_{k+1}} \sum_{i=1}^{6} Y_{i,k+1} - \frac{1}{n_{k+1}} \sum_{i=1}^{6} Z_{i,k+1}, \tag{5}$$

where:

$$X_{k+1} = \frac{\Lambda}{N_{k+1}} \left(\frac{dN}{dt} \right)_{t_{k+1}} + \beta_{eff}, \tag{6}$$

$$Y_{i,k+1} = Y_{i,k} e^{-\lambda_i \Delta t}, \tag{7}$$

$$Z_{i,k+1} = Z_{i,k} e^{-\lambda_i \Delta t} + \lambda_i \beta_i e^{-\lambda_i t_{k+1}} \int_{t_k}^{t_{k+1}} N(t') e^{\lambda_i t'} dt', \tag{8}$$

with $\Delta t = t_{k+1} - t_k$, and

$$\left(\frac{dN}{dt} \right)_{t_{k+1}} = \frac{N_{k+1} - N_k}{\Delta t}. \tag{9}$$

Assuming also that $N(t)$ varies linearly inside of the interval Δt as $N(t) = a + bt$, the integral in Eq. (8) yields:

$$\int_{t_k}^{t_{k+1}} N(t') e^{\lambda_i t'} dt' = \frac{e^{\lambda_i t_{k+1}}}{\lambda_i} \left(N_{k+1} - \frac{b}{\lambda_i} \right) - \frac{e^{\lambda_i t_k}}{\lambda_i} \left(N_k - \frac{b}{\lambda_i} \right) \tag{10}$$

and consequently:

$$e^{-\lambda_i t_{k+1}} \int_{t_k}^{t_{k+1}} N(t') e^{\lambda_i t'} dt' = \left\{ \frac{1}{\lambda_i} \left(N_{k+1} - \frac{b}{\lambda_i} \right) - \frac{e^{-\lambda_i \Delta t}}{\lambda_i} \left(N_k - \frac{b}{\lambda_i} \right) \right\}. \tag{11}$$

Finally, Eq. (8) for Z_{ik+1} can be written as:

$$Z_{i,k+1} = Z_{i,k} e^{-\lambda_i \Delta t} + \beta_i \left\{ \left(N_{k+1} - \frac{b}{\lambda_i} \right) - e^{-\lambda_i \Delta t} \left(N_k - \frac{b}{\lambda_i} \right) \right\} \tag{12}$$

The recursive way to solve Eq, (3) is noted in $Y_{i,k+1}$ and $Z_{i,k+1}$ which depends on their previous values. The initialization of the algorithm is made considering the reactor critical at the beginning of the process or $t_0 = 0$. In this case, the initial values for the variables X_k, Y_k, and Z_k are given by:

$$X_0 = \beta_{eff} \tag{13}$$

$$Y_{i,0} = (\beta_i / \Lambda) N(0), \tag{14}$$

and

$$Z_{i,0} = 0 \tag{15}$$

This is the recursive process for the determination of the reactivity in the inverse kinetic method employed in the IPEN/MB-01 reactor. The reactivity at instant t_{k+1} is obtained from the previous data at instant t_k. Eq. (5) for ρ_{k+1} in conjunction with Eqs. (6) through (15) constitutes the final set of equations to be employed in this recursive process. This whole process is referred to as the IPEN/MB-01 reactivity meter.

The IPEN/MB-01 reactivity meter runs in a microcomputer, and it was written in a graphical language LABVIEW. Its basic input data are the effective kinetics parameters for its core and the detectors signals which arises from the detector measurement chain composed of detectors operating in current mode (compensated ionization chambers), an electrometer (Keithley 614), and a GPIB board. This measurement chain runs in an acquisition rate of one sample per second.

Table 1
Inferred delayed neutron abundances $a_i = (\beta_i / \beta_{eff})$ and their corresponding uncertainties.

Delayed Neutron Group i	CPSD a_i	APSD1$^{(*)}a_i$	APSD2$^{(*)}a_i$
1	0.0374 ± 0.0007	0.0363 ± 0.0007	0.0381 ± 0.0007
2	0.1919 ± 0.0078	0.1946 ± 0.0077	0.1963 ± 0.0071
3	0.1839 ± 0.0132	0.1981 ± 0.0136	0.1804 ± 0.0123
4	0.4068 ± 0.0132	0.3931 ± 0.0133	0.4051 ± 0.0123
5	0.1147 ± 0.0066	0.1135 ± 0.0068	0.1182 ± 0.0063
6	0.0654 ± 0.0030	0.0644 ± 0.0029	0.0619 ± 0.0028

(*) APSD1 and APSD2 refer, respectively to the Auto Power Spectral Density for Detector 1 and 2.

2.2. The reactivity meter uncertainty analyses

The reactivity uncertainty analysis can be performed considering the general equation for the propagation of the associated uncertainties (ANSI, 1997). Let x_i be an independent or correlated set of variables and $w(x_i)$ a dependent function of this set of variables. Accordingly, the uncertainty of $w(x_i)$ is:

$$\sigma_w^2 = \sum_{i=1}^{n} \left(\frac{\partial w}{\partial x_i} \right)^2 \cdot \sigma_{x_i}^2 + 2 \cdot \sum_{j=1}^{n} \sum_{i>j}^{n} \frac{\partial w}{\partial x_i} \cdot \frac{\partial w}{\partial x_j} \cdot \sigma_{x_i} \cdot \sigma_{x_j} \cdot corr(x_i, x_j), \tag{16}$$

where σ_w is the uncertainty of $w(x_i)$, x_i is a generic independent variable, σ_i is the uncertainty of x_i and $corr(x_i, x_j)$ is the correlation matrix for x_i and x_j.

The reactivity uncertainty is determined employing Eq. (16). The dependent function $w(x_i)$ is replaced by the reactivity (ρ) and the generic independent variables x_i are replaced by the components of the Kinetics Parameter Data Vector (*KPDV*) defined as:

$$KPDV = (\Lambda, \lambda_1, \cdots, \lambda_6, \beta_1, \cdots, \beta_6) \tag{17}$$

The source of the effective kinetics parameter data vector and their uncertainties as well needed to get the reactivity and its uncertainty arise from IPEN(MB01)-LWR-RESR-021. This evaluation derived three complete set of experimental kinetics parameters to infer reactivities as a function of the reactor period employing the Inhour Equation (Bell and Glasstone, 1979). This goal was accomplished employing a least squares approach to fit the available spectral densities measured at the IPEN/MB-01 reactor; namely the APSD (Auto Power Spectral Density) and the CPSD (Cross Power Spectral Density). These raw data (APSD and CPSD data) arise from the experiments performed during the years 2005 through 2006 at the IPEN/MB-01 reactor employing a macroscopic noise technique in the very low frequency range (<1.0 Hz) (Diniz and dos Santos, 2006). The parameters to be fitted were the delayed neutron abundances (β_i / β_{eff}) and its decay constant (λ_i.) in six groups of delayed neutrons. The first decay constant (λ_1) was kept fixed in the least squares fitting processes. Its value arises from (dos Santos et al., 2006b) and it is also available in Table 3.6.5-1 of IPEN(MB01)-LWR-RESR-001; (kinetics parameters evaluation) (dos Santos et al., 2012). A modified version of the least squares code DELAY (Spriggs, 1993) based on the Levenberg-Marquardt algorithm (Press et al., 1992) was employed to cope with this task. The least squares approaches were successfully carried out and

Table 2
Inferred delayed neutron decay constant (s^{-1}) and their corresponding uncertainties.

Delayed Neutron Group i	CPSD λ_i (s^{-1})	APSD1 λ_i (s^{-1})	APSD2 λ_i(s^{-1})
1	0.012456 ± 0.000031(*)	0.012456 ± 0.000031(*)	0.012456 ± 0.000031(*)
2	0.0314 ± 0.0025	0.0309 ± 0.0025	0.0315 ± 0.0021
3	0.1096 ± 0.0039	0.1129 ± 0.0038	0.1110 ± 0.0045
4	0.3052 ± 0.0043	0.3044 ± 0.0047	0.3078 ± 0.0046
5	1.070 ± 0.031	1.048 ± 0.032	1.083 ± 0.029
6	3.21 ± 0.10	3.288 ± 0.087	2.6001 ± 0.086

(*) From (dos Santos et al., 2006b) and from Table 3.6.5–1 of IPEN(MB01)-LWR-RESR-001; kinetics parameters evaluation (dos Santos, 2012).

Table 3
Inferred delayed neutron fraction (β_i) and corresponding uncertainties for the CPSD case.

Delayed Neutron Group i	β_i	$\sigma_{\beta_i}^{corr}$	$\sigma_{\beta_i}^{uncorr}$	σ_{β_i}
1	2.723E-04	5.25E-06	1.82E-06	5.56E-06
2	1.460E-03	5.78E-05	9.73E-06	5.86E-05
3	1.486E-03	1.02E-04	9.91E-06	1.02E-04
4	2.948E-03	1.02E-04	1.97E-05	1.04E-04
5	8.513E-04	5.10E-05	5.68E-06	5.13E-05
6	4.830E-04	2.18E-05	3.22E-06	2.20E-05

Table 4
Inferred delayed neutron fraction ($\boldsymbol{\beta_i}$) and corresponding uncertainties for the APSD1 case.

Delayed Neutron Group i	β_i	$\sigma_{\beta_i}^{corr}$	$\sigma_{\beta_i}^{uncorr}$	σ_{β_i}
1	2.723E-04	5.25E-06	1.82E-06	5.56E-06
2	1.460E-03	5.78E-05	9.73E-06	5.86E-05
3	1.486E-03	1.02E-04	9.91E-06	1.02E-04
4	2.948E-03	1.02E-04	1.97E-05	1.04E-04
5	8.513E-04	5.10E-05	5.68E-06	5.13E-05
6	4.830E-04	2.18E-05	3.22E-06	2.20E-05

the outcoming uncertainties were appropriate for a benchmark problem to test the adequacy of the delayed neutron parameters available in several nuclear data libraries. The procedure developed in the IPEN (MB01)-LWR-RESR-021 evaluation to infer the effective delayed neutron parameters relied only in experimental data and can be considered purely experimental. The procedure did not employ any sort of calculated correction factor or similar quantities. The main results arising from the IPEN(MB01)-LWR-RESR-021 least squares fitting processes of each spectral density are given in a six-delayed group model in Tables 1 and 2, respectively for the delayed neutron abundances and its decay constants.

According to IPEN(MB01)-LWR-RESR-021, the delayed neutron faction (β_i) for group i was found as:

$$\beta_i = \beta_{eff} a_i, \tag{18}$$

where a_i is from Table 1 and β_{eff} and its corresponding uncertainty are from Table 3.6.5-1 of IPEN(MB01)-LWR-RESR-001; kinetics parameter evaluation (dos Santos, 2012). β_{eff} and $\sigma_{\beta_{eff}}$ are, respectively, equal to 0.00750 and 0.00005. The delayed neutron abundances a_i and the effective delayed neutron fraction (β_{eff}) are assumed to be uncorrelated due to their different origins. Consequently, the β_i uncertainty was split into two components. The correlated component ($\sigma_{\beta_i}^{corr}$) given by $\beta_{eff}\sigma_{a_i}$ and the uncorrelated component ($\sigma_{\beta_i}^{uncorr}$) given by $a_i\sigma_{\beta_{eff}}$. The total uncertainty on β_i is given by:

$$\sigma_{\beta_i} = \sqrt{\left(\sigma_{\beta_i}^{corr}\right)^2 + \left(\sigma_{\beta_i}^{uncorr}\right)^2} \tag{19}$$

Table 5
Inferred delayed neutron fraction ($\boldsymbol{\beta_i}$) and corresponding uncertainties for the APSD2 case.

Delayed Neutron Group i	β_i	$\sigma_{\beta_i}^{corr}$	$\sigma_{\beta_i}^{uncorr}$	σ_{β_i}
1	2.858E-04	5.25E-06	2.67E-06	5.89E-06
2	1.472E-03	5.33E-05	1.37E-05	5.50E-05
3	1.353E-03	9.23E-05	1.26E-05	9.32E-05
4	3.038E-03	9.23E-05	2.84E-05	9.66E-05
5	8.865E-04	4.73E-05	8.27E-06	4.80E-05
6	4.643E-04	2.10E-05	4.33E-06	2.14E-05

Tables 3 through 5 show the final results for the delayed neutron fraction (β_i) for group i and its respective uncertainty, respectively for the spectral densities CPSD, APSD1, and APSD2. According to (ANSI, 1997) the β_i uncertainties are classified for each spectral density as Type B.

Tables 3 through 5 in conjunction with the prompt neutron generation time (Λ= (31.96 ± 1.06) μs) from IPEN(MB01)-LWR-RESR-001 (kinetics evaluation) (dos Santos et al., 2012) form a complete set of kinetic parameters to be employed in the reactivity meter with uncertainties developed in this work.

The correlation matrix for the components of the Kinetic Parameter Data Vector is given in Table 6. In this matrix, the prompt neutron generation time ($\boldsymbol{\Lambda}$) and the first decay constant ($\boldsymbol{\lambda_1}$) are assumed to be uncorrelated to each other and to the remaining delayed neutron parameters. The correlation among β_i, with i equals to 1 through 6, and λ_i, with i equals to 2 through 6 arises from (dos Santos and Diniz, 2020).

Since the basic input data required for the IPEN/MB-01 reactivity meter with uncertainties are known and well understood, the question of the determination of the reactivity uncertainty reduces to the one of obtaining the reactivity derivatives to the components of the Kinetics Parameter Data Vector. These derivatives can be found from Eq. (5) as:

$$\frac{\partial \rho_{k+1}}{\partial \lambda_i} = \frac{\partial X_{k+1}}{\partial \lambda_i} - \frac{\Lambda}{n_{k+1}}\frac{\partial Y_{i,k+1}}{\partial \lambda_i} - \frac{1}{n_{k+1}}\frac{\partial Z_{i,k+1}}{\partial \lambda_i}, \tag{20}$$

$$\frac{\partial \rho_{k+1}}{\partial \beta_i} = \frac{\partial X_{k+1}}{\partial \beta_i} - \frac{\Lambda}{n_{k+1}}\frac{\partial Y_{i,k+1}}{\partial \beta_i} - \frac{1}{n_{k+1}}\frac{\partial Z_{i,k+1}}{\partial \beta_i}, \tag{21}$$

where $i = 1, \cdots 6$ in Eqs. (20) and (21) and

$$\frac{\partial \rho_{k+1}}{\partial \Lambda} = \frac{\partial X_{k+1}}{\partial \Lambda} - \frac{\Lambda}{n_{k+1}}\sum_{i=1}^{6}\frac{\partial Y_{i,k+1}}{\partial \Lambda} - \frac{1}{n_{k+1}}\sum_{i=1}^{6} Y_{i,k+1} - \frac{1}{n_{k+1}}\sum_{i=1}^{6}\frac{\partial Z_{i,k+1}}{\partial \Lambda} \tag{22}$$

The derivatives of X_{k+1}, $Y_{i,k+1}$, and $Z_{i,k+1}$ to the components of the Kinetics Parameter Data Vector can be found, respectively from Eqs. (6) through (8) as:

$$\frac{\partial X_{k+1}}{\partial \lambda_i} = 0 \tag{23}$$

$$\frac{\partial X_{k+1}}{\partial \beta_i} = 1 \tag{24}$$

$$\frac{\partial X_{k+1}}{\partial \Lambda} = \frac{1}{n_{k+1}}\left(\frac{dN}{dt}\right)_{t_{k+1}} \tag{25}$$

$$\frac{\partial Y_{i,k+1}}{\partial \lambda_i} = \frac{\partial Y_{i,k}}{\partial \lambda_i}e^{-\lambda_j \Delta t} - Y_{i,k}\Delta t e^{-\lambda_i \Delta t}, \tag{26}$$

$$\frac{\partial Y_{i,k+1}}{\partial \beta_i} = \frac{\partial Y_{i,k}}{\partial \beta_i}e^{-\lambda_i \Delta t} \tag{27}$$

$$\frac{\partial Y_{i,k+1}}{\partial \Lambda} = \frac{\partial Y_{i,k}}{\partial \Lambda}e^{-\lambda_i \Delta t} \tag{28}$$

Table 6
The correlation matrix for the effective kinetics parameters.

	Λ	β_1	β_2	β_3	β_4	β_5	β_6	λ_1	λ_2	λ_3	λ_4	λ_5	λ_6
Λ	1	0	0	0	0	0	0	0	0	0	0	0	0
β_1	0	1	−0.993	−0.846	−0.725	−0.105	−0.134	0	0.993	0.848	0.732	0.106	0.134
β_2	0	−0.993	1	0.901	0.784	0.156	0.169	0	−1	−0.902	−0.79	−0.157	−0.169
β_3	0	−0.846	0.901	1	0.942	0.374	0.309	0	−0.902	−1	−0.945	−0.375	−0.309
β_4	0	−0.725	0.784	0.942	1	0.621	0.491	0	−0.786	−0.942	−1	−0.622	−0.491
β_5	0	−0.105	0.156	0.374	0.621	1	0.89	0	−0.158	−0.374	−0.616	−1	−0.89
β_6	0	−0.134	0.169	0.309	0.491	0.89	1	0	−0.17	−0.309	−0.488	−0.891	−1
λ_1	0	0	0	0	0	0	0	1	0	0	0	0	0
λ_2	0	0.993	−1	−0.902	−0.786	−0.158	−0.17	0	1	0.903	0.792	0.159	0.171
λ_3	0	0.848	−0.902	−1	−0.942	−0.374	−0.309	0	0.903	1	0.945	0.375	0.309
λ_4	0	0.732	−0.79	−0.945	−1	−0.616	−0.488	0	0.792	0.945	1	0.617	0.488
λ_5	0	0.106	−0.157	−0.375	−0.622	−1	−0.891	0	0.159	0.375	0.617	1	0.891
λ_6	0	0.134	−0.169	−0.309	−0.491	−0.89	−1	0	0.171	0.309	0.488	0.891	1

$$\frac{\partial Z_{i,k+1}}{\partial \lambda_i} = \frac{\partial Z_{i,k}}{\partial \lambda_i} e^{-\lambda_i \Delta t} - Z_{i,k} \Delta t e^{-\lambda_i \Delta t} + A + B + C \tag{29}$$

where:

$$\mathrm{A} = +\beta_i \frac{(1-\lambda_i t_{k+1})}{\lambda_i} \left\{ \left(N_{k+1} - \frac{b}{\lambda_i} \right) - e^{-\lambda_i \Delta t} \left(N_k - \frac{b}{\lambda_i} \right) \right\} \tag{30}$$

$$\mathrm{B} = +\beta_i \left\{ \left(\frac{\lambda_i t_{k+1} - 1}{\lambda_i} \right) \left(N_{k+1} - \frac{b}{\lambda_i} \right) + \frac{b}{{\lambda_i}^2} \right\}, \tag{31}$$

$$\mathrm{C} = -\beta_i e^{-\lambda_i \Delta t} \left\{ \left(\frac{\lambda_i t_k - 1}{\lambda_i} \right) \left(N_k - \frac{b}{\lambda_i} \right) + \frac{b}{{\lambda_i}^2} \right\}, \tag{32}$$

$$\frac{\partial Z_{i,k+1}}{\partial \beta_i} = \frac{\partial Z_{i,k}}{\partial \beta_i} e^{-\lambda_i \Delta t} + \left\{ \left(N_{k+1} - \frac{b}{\lambda_i} \right) - e^{-\lambda_i \Delta t} \left(N_k - \frac{b}{\lambda_i} \right) \right\} \tag{33}$$

and

$$\frac{\partial Z_{i,k+1}}{\partial \Lambda} = \frac{\partial Z_{i,k}}{\partial \Lambda} e^{-\lambda_i \Delta t} \tag{34}$$

The derivatives of X_{k+1}, $Y_{i,k+1}$, and $Z_{i,k+1}$ at the initial conditions can be found, respectively from Eqs. (13) through (15) in a straightforward fashion.

The delayed neutron data available in Tables 2 through 5 in conjunction with the known value of the prompt neutron generation time $\Lambda = (31.96 \pm 1.06)$ μs) are the starting point to get the reactivity uncertainties in the IPEN/MB-01 reactivity meter. The procedure adopted here to get the reactivity uncertainties as a function of time follows closely to that described in IPEN(MB01)-LWR-RESR-021.

The reactivity uncertainty at a generic time step t_{k+1} arising from each spectral density is split into correlated ($\sigma^{corr}_{\rho_{k+1}}$) and uncorrelated ($\sigma^{uncorr}_{\rho_{k+1}}$) contributions and they are given by:

$$\sigma^{corr}_{\rho_{k+1}} = \sqrt{\sum_{i=1}^{6} \left(\frac{\partial \rho_{k+1}}{\partial \beta_i} \right)^2 \cdot \left(\sigma^{corr}_{\beta_i} \right)^2 + \sum_{i=2}^{6} \left(\frac{\partial \rho_{k+1}}{\partial \lambda_i} \right)^2 \cdot \sigma^2_{\lambda_i} + Cov^{\beta}_{\rho_{k+1}} + Cov^{\lambda}_{\rho_{k+1}} + Cov^{\beta\lambda}_{\rho_{k+1}}}, \tag{35}$$

where

$$Cov^{\beta}_{\rho_{k+1}} = 2 \cdot \sum_{i=1}^{6} \sum_{j=i+1}^{6} \frac{\partial \rho_{k+1}}{\partial \beta_i} . \frac{\partial \rho_{k+1}}{\partial \beta_j} . \sigma^{corr}_{\beta_i} . \sigma^{corr}_{\beta_j} . Corr(i+1, j+1) \tag{36}$$

$$Cov^{\lambda}_{\rho_{k+1}} = 2 \cdot \sum_{i=2}^{6} \sum_{j=i+1}^{6} \frac{\partial \rho_{k+1}}{\partial \lambda_i} . \frac{\partial \rho_{k+1}}{\partial \lambda_j} . \sigma_{\lambda_i} . \sigma_{\lambda_j} . Corr(i+1, j+7), \tag{37}$$

$$Cov^{\beta\lambda}_{\rho_{k+1}} = 2 \cdot \sum_{i=1}^{6} \sum_{j=i+1}^{6} \frac{\partial \rho_{k+1}}{\partial \beta_i} . \frac{\partial \rho_{k+1}}{\partial \lambda_j} . \sigma^{corr}_{\beta_i} . \sigma_{\lambda_j} . Corr(i+1, j+7), \tag{38}$$

and

$$\sigma^{uncorr}_{\rho_{k+1}} = \sqrt{\left(\frac{\partial \rho_{k+1}}{\partial \Lambda} \right)^2 \cdot \sigma^2_{\Lambda} + \left(\frac{\partial \rho_{k+1}}{\partial \lambda_1} \right)^2 \cdot \sigma^2_{\lambda_1} + \sum_{i=1}^{6} \left(\frac{\partial \rho_{k+1}}{\partial \beta_i} \sigma^{uncorr}_{\beta_i} \right)^2} \tag{39}$$

The final reactivity uncertainty for each spectral density is found as:

$$\sigma_{\rho_{k+1}} = \sqrt{\left(\sigma^{corr}_{\rho_{k+1}} \right)^2 + \left(\sigma^{uncorr}_{\rho_{k+1}} \right)^2} \tag{40}$$

Eq. (40) for the final total reactivity uncertainty ($\sigma_{\rho_{k+1}}$) in conjunction with Eqs. (23) through (34) for the derivatives of X_{k+1}, $Y_{i,k+1}$, and $Z_{i,k+1}$, with Eqs. (35) through (38) for $\sigma^{corr}_{\rho_{k+1}}$, and with Eq. (39) for $\sigma^{uncorr}_{\rho_{k+1}}$ form a complete set of equations for the determination of the reactivity uncertainty as a function of time.

The numerical approach to get the reactivity uncertainties runs sequentially to that implement in the IPEN/MB-01 reactivity meter. The whole set is referred to as IPEN/MB-01 reactivity meter with uncertainties.

3. The IPEN/MB-01 reactivity meter with uncertainties validation

The IPEN/MB-01 reactivity meter with uncertainties given by described in Sections 2.1 and 2.2 is validated against the corresponding results obtained from the Inhour equation (Bell and Glasstone, 1979). According to the Inhour equation the reactivity in a six delayed neutron group model for a given reactor period T is given by:

$$\rho = \frac{\Lambda}{T} + \sum_{i=1}^{6} \frac{\beta_i}{1 + \lambda_i T} \tag{41}$$

The Inhour equation uncertainty analysis can be performed employing the same procedure as that described in Section 2.2. The Inhour equation is considered for selected reactor periods and employs the whole set of kinetics parameters given in Tables 3 through 5 in

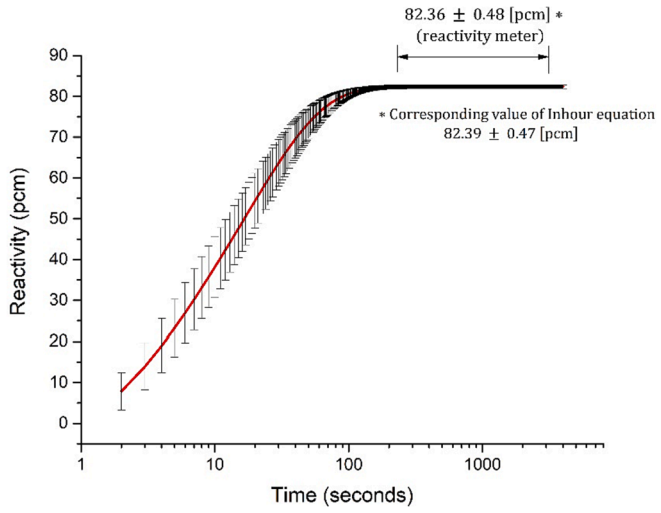

Fig. 1. The reactivity results for the period equal to 80 s.

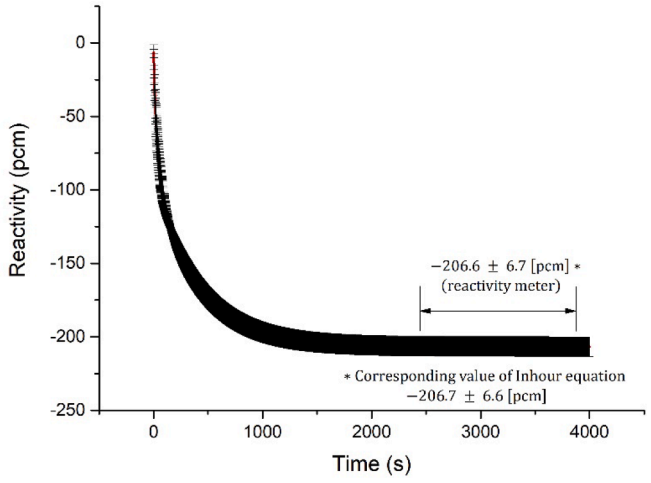

Fig. 2. The reactivity results for the period equal to −100 s.

conjunction with the known prompt neutron generation time ($\Lambda = (31.96 \pm 1.06)\,\mu s$). The comparisons are made for each set of kinetic parameters giving in these tables. Here the time dependence is ignored, the reactivity uncertainty is given by Equation (40), and σ_{corr} and σ_{uncorr} are given by Eqs. (35) through (39) as before. The reactivity derivatives to be employed in this set of equations are now given by:

$$\frac{\partial \rho}{\partial \Lambda} = \frac{1}{T} \tag{42}$$

$$\frac{\partial \rho}{\partial \beta_i} = \frac{1}{(1+\lambda_i \cdot T)}, \text{ and} \tag{43}$$

$$\frac{\partial \rho}{\partial \lambda_i} = -\frac{\beta_i \cdot T}{(1+\lambda_i T)^2}. \tag{44}$$

The consistency between the inverse kinetics model with uncertainties developed in this paper and that of the Inhour equation model given by Eq. (41) can be made by assuming that $N(t)$ in Eq. (3) is given by:

$$N(t) = Ae^{t/T}, \tag{45}$$

Figs. 1 and 2 show these model comparisons, respectively for periods of 80 and −100 s. The reactivity data were built considering the kinetics parameters for both models from the CPSD case and the correlated uncertainties ($\sigma_{\beta_i}^{corr}$) as given in Table 4. Eqs. (35) through (38) are considered accordingly and the final reactivity uncertainty is just the correlated component. Figs. 1 and 2 show the reactivity calculated by the reactivity meter model starts at zero because by hypothesis this is the initial condition of a critical reactor. Also, these figures show that the inferred reactivity has a plateau region and stabilizes, respectively at times longer than nearly 120 and 3000 s for the positive and negative periods. The average reactivity ($\overline{\rho}$) from the reactivity meter in this time plateau interval is determined by a weighted average method (Zhang, 2006) as:where A is an arbitrary constant, and t, and T have the same meaning as before.

$$\overline{\rho} = \frac{\sum_{i=1}^{NP} \rho_i \cdot w_i}{\sum_{i=1}^{NP} w_i}, \tag{46}$$

where NP is the total number de points in a selected time portion of the plateau interval, ρ_i, and w_i are, respectively the reactivity and the weighting factor both at time t_i. The weighting factor (w_i) for this application is giving by:

$$w_i = \frac{1}{(\sigma_{\rho_i})^2}, \tag{47}$$

where σ_{ρ_i} is the uncertainty of the reactivity ρ_i at a generic time t_i and the uncertainty in $\overline{\rho}$ is giving by:

$$\sigma_{\overline{\rho}} = \frac{\sqrt{NP}}{\sqrt{\sum_{i=1}^{NP} w_i}} \tag{48}$$

The reason for the factor $\sqrt{NP}$ in the numerator of Eq. (48) is to eliminate the statistical component that is implicit in the weighting average process. In the limiting case where all uncertainties are equal, (σ) for example, the weighting average method will give rise to an uncertainty in the parameter under consideration of $\sigma/\sqrt{M}$, where M is the number of samples considered. This uncertainty is referred to as *the standard deviation of the mean*. If Eqs. (46) through (48) were applied in

Table 7
Comparison between reactivity meter with uncertainties and Inhour equation.

Period (s)	ρ(pcm)		σ_ρ^{corr} pcm)		σ_ρ^{uncorr}(pcm)		σ_ρ(pcm)	
	Inhour Equation	Reactivity Meter	Inhour Equation	Reactivity Meter	Inhour Equation	Reactivity Meter	Inhour Equation	Reactivity Meter
CPSD								
−100	−206.7	−206.6	6.6	6.7	1.46	1.46	6.8	6.9
80	82.39	82.36	0.47	0.48	0.31	0.31	0.57	0.57
APSD1								
−100	−206.0	−206.2	7.1	7.2	1.7	1.4	7.3	7.3
80	83.31	83.34	0.53	0.53	0.32	0.32	0.62	0.62
APSD2								
−100	−209.4	−210.0	5.94	5.94	1.51	1.50	6.1	6.1
80	82.98	82.94	0.40	0.39	0.45	0.44	0.60	0.59

Table 8
Relative contributions of the of the reactivity uncertainty for the CPSD case.

Period (s)	$RC_{\beta^{corr}}$	$RC_{\beta^{uncorr}}$	$RC_{\beta\lambda}$	RC_{λ}	RC_{λ_1}	RC_{Λ}
−100	0.09	0.00	−0.66	1.53	0.04	0.00
80	23.33	0.31	−48.37	25.73	0.00	0.00

this case the final uncertainty would be σ. This is the desired result for uncertainties type B.

The uncertainties in the reactivities as a function of time inferred by the reactivity meter are not of statistical nature. They are classified as Type B. Adopting the validity of Eqs. (46) through (48), the comparison of the results of the reactivity meter with uncertainties to those of the Inhour Equation is not only possible but also as shown in Figures 1 and 2 it comes into a very good agreement.

Table 7 shows a complete comparison between these two reactivity models. Now, the comparison is made for all spectral densities as well as for the correlated, uncorrelated, and total reactivity uncertainties. Also here, the agreement between these two models is very good and reinforces the validity of the whole procedure for the development of the reactivity meter with uncertainties.

To give some insight on the relative contribution of the kinetics parameters employed to get the reactivity uncertainties consider Eq. (40) for a generic reactivity ρ and Equations (35) and (39), respectively for the determination of σ_{ρ}^{corr} and σ_{ρ}^{uncorr}. Now let the derivatives of the reactivity to the kinetics parameters in Equations (41) be given by Equations (42) through (44) i.e., the Inhour Equation model. Furthermore, let the relative contributions of the input kinetics parameters to get the reactivity uncertainties be grouped into six broad categories defined as:

1) the relative contribution of the correlated part of all the delayed neutron fractions ($\sigma_{\beta_i}^{corr}$'s) and the correlation among them given by:

$$RC_{\beta^{corr}} = \frac{\sum_{i=1}^{ND}\left(\frac{\partial\rho}{\partial\beta_i}\right)^2\cdot\left(\sigma_{\beta_i}^{corr}\right)^2 + 2\cdot\sum_{i=1}^{ND}\sum_{j=i+1}^{ND}\frac{\partial\rho}{\partial\beta_i}\cdot\frac{\partial\rho}{\partial\beta_j}\cdot\sigma_{\beta_i}^{corr}\cdot\sigma_{\beta_j}^{corr}\cdot Corr(i+1,j+1)}{(\sigma_{\rho})^2}, \tag{49}$$

2) the relative contribution of the uncorrelated part of the delayed neutron fraction given by:

$$RC_{\beta^{uncorr}} = \frac{\sum_{i=1}^{ND}\left(\frac{\partial\rho}{\partial\beta_i}\sigma_{\beta_i}^{uncorr}\right)^2}{(\sigma_{\rho})^2} \tag{50}$$

3) the relative contribution of all the terms that are part of the correlation among β_i and λ_j, being i from 1 to ND, and j from 2 to ND given by:

$$RC_{\beta\lambda} = 2\cdot\frac{\sum_{i=1}^{ND}\sum_{j=i+1}^{ND}\frac{\partial\rho}{\partial\beta_i}\cdot\frac{\partial\rho}{\partial\lambda_j}\cdot\sigma_{\beta_i}^{corr}\cdot\sigma_{\lambda_j}\cdot Corr(i+1,j+ND+1)}{(\sigma_{\rho})^2}, \tag{51}$$

4) the relative contribution of all terms involving the decay constants λ_2 through λ_6 and the correlation among them given by:

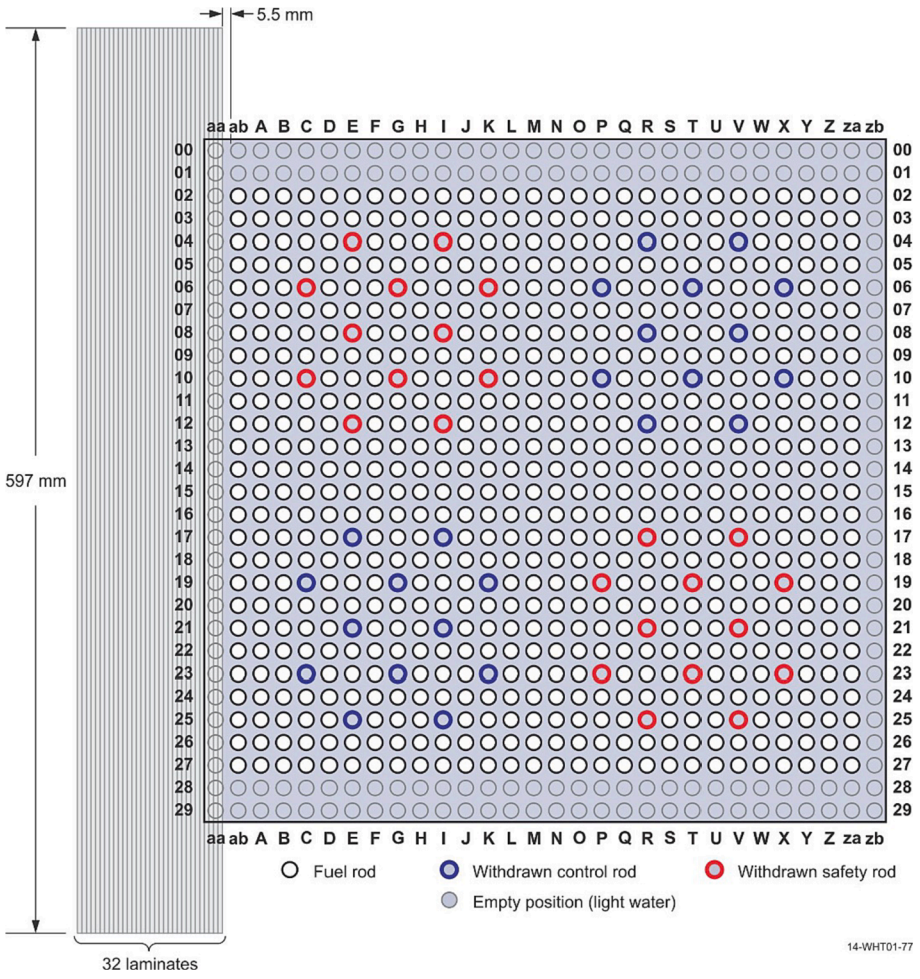

Fig. 3. Experimental core configuration for the case of 32 nickel plates.

$$RC_{\lambda} = \frac{\sum_{i=2}^{ND}\left(\frac{\partial\rho}{\partial\lambda_i}\right)^2 \cdot(\sigma_{\lambda_i})^2 + 2\cdot\sum_{i=2}^{ND}\sum_{j=i+1}^{ND}\frac{\partial\rho}{\partial\lambda_i}.\frac{\partial\rho}{\partial\lambda_j}.\sigma_{\lambda_i}.\sigma_{\lambda_j}.Corr(i+1,j+ND+1)}{(\sigma_{\rho})^2}, \tag{52}$$

5) the relative contribution of the first decay constant (λ_1) given by:

$$RC_{\lambda_1} = \frac{\left(\frac{\partial\rho}{\partial\lambda_1}\right)^2 \cdot\sigma_{\lambda_1}^2}{(\sigma_{\rho})^2}, \text{ and} \tag{53}$$

6) the relative contribution of the prompt neutron generation time (Λ) given by:

$$RC_{\wedge} = \frac{\left(\frac{\partial\rho}{\partial\wedge}\right)^2 \bullet\sigma_{\wedge}^2}{(\sigma_{\rho})^2} \tag{54}$$

Note that these relative contributions consider all the terms inside of the square root of Equation (40) and σ_{ρ} is the total reactivity uncertainty also given by this equation. Moreover, the sum of all these six category contributions is equal to 1.0.

Table 8 shows the values for each of these 6 category contributions for the two periods of Table 7. Only the CPSD case results are shown in this table. The APSD1 and APSD2 results follow basically the same tendency.

Table 8 makes the analyses of the uncertainty in the reactivity more understandable. Initially, the first decay constant and the prompt neutron generation time play practically no role for the determination of the reactivity uncertainty for both periods of Table 8. The first decay constant is very important for the determination of the reactivity uncertainty when the period is very close to $1/\lambda_1$. Conversely, the prompt neutron generation time (Λ) is very important for short periods when the fission chain reaction is controlled by the prompt neutrons. RC_{β}., both correlated and uncorrelated part practically is not important for the negative period, but it is very important for the positive one. There are huge cancellations in the uncertainty analysis mainly for $RC_{\beta\lambda}$ and the sum of RC_{λ} and RC_{β}. The contribution of β_i and λ_i individually given by $RC_{\beta}andRC_{\lambda}$ are positive and the contributions of the correlation among these two quantities given by $RC_{\beta\lambda}$ are negative. These explain good part of the reason why the uncertainty in the inferred reactivity is reduced when correlation is taken into consideration. These apply to both negative and positive periods.

4. The reactivity uncertainty analyses application

The reactivity meter with uncertainties model developed in Sections 2.1 and 2.2 was applied to a practical case considering the benchmark IPEN(MB01)-LWR-RESR-015 (dos Santos et al., 2014). This benchmark was approved by the IRPhE (International Reactor Physics Experiments) and addressed the evaluation of the heavy reflector experiment composed of Nickel plates in the west face of the IPEN/MB-01 reactor. The Nickel heavy reflector evaluation comprise a set of critical configurations employing the standard 28 × 26-fuel-rod configuration. Up to 32 plates, approximately 3.0-mm-thick each, were used in the experiment. Figure 3 shows the experimental core configuration for the case of 32 Nickel Plates. A complete description of the IPEN/MB-01 reactor core and of the specific experiment under consideration here can be found in IPEN(MB01)-LWR-RESR-015. More details can be found several other benchmark publications available in the handbooks of the NEA/OECD projects ICSBEP and IRPhE.

The quantities measured in the Nickel heavy reflector experiments were the control bank critical positions, the total reactivity (ρ) relative to the case without Nickel plates and the reactivity gain (Δρ) between the case under consideration and the previous case. Eighteen cases were evaluated and approved to be include in the IRPhE handbook.

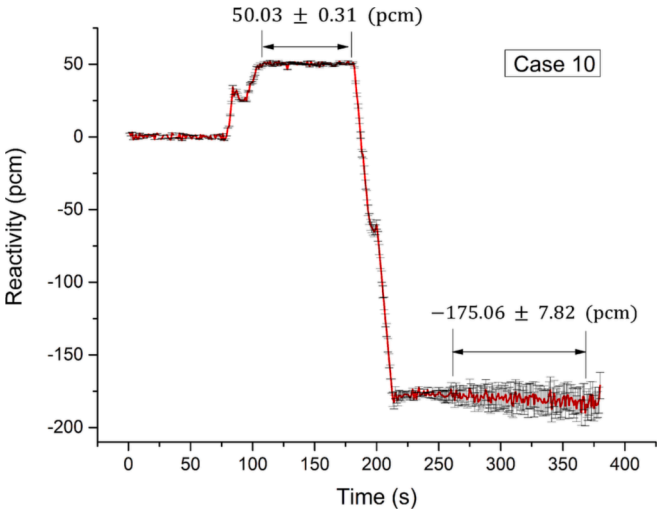

Fig. 4. CPSD reactivity measurements for Case 10.

The cases under analyses for the application of the reactivity meter with uncertainties were Case 2 employing 1 Nickel plate, Case 10 employing 9 Nickel plates both for the total reactivity and the reactivity gain of Cases 10 and 14. The reactivity gain of Case 10 is relative to Case 9 which contains 8 Nickel plates. Case 14 employs 18 Nickel plates and the reactivity gain is relative to Case 13 which contains 15 Nickel plates.

The reactivity measuring procedure consists of making the IPEN/MB-01 reactor critical for the specific number of Nickel plates under consideration followed by a rapid control bank position changes either to the critical positions of the case without Nickel plates for the total reactivity or to the critical positions of the previous case for the reactivity gain. The whole set of experimental values for all evaluated cases are given in Table 2.4.1–1 of IPEN(MB01)-LWR-RESR-015.

The main objective here is to verify the validity of the hypotheses made in this evaluation to get the experimental reactivity and its uncertainty. According to the IPEN(MB01)-LWR-RESR-015 evaluation, the uncertainty in the average experimental reactivity was given by:

$$\sigma_{\rho} = \frac{\{|\rho^{+} - \rho| + |\rho^{-} - \rho|\}}{2 \bullet \sqrt{3}}, \tag{55}$$

where ρ is the nominal value of the inferred reactivity, i.e., inferred with the nominal values of the effective delayed neutron fraction, decay constants and the prompt neutron generation time. ρ^{-} is the inferred reactivity when the uncertainty of the kinetic parameters is subtracted to their corresponding nominal values. Conversely, ρ^{+} is the inferred reactivity when the uncertainty of the kinetic parameters is added to their corresponding nominal values. The $\sqrt{3}$ factor was recommended by the experimentalists since the relative abundances and the decay constants were inferred employing only the spectral density CPSD. Two APSD's were available at the time of the IPEN(MB01)-LWR-RESR-015 evaluation but they were not subject to the fitting process to get the delayed neutron parameters. The inclusion of the results of the fitting for the other two APSD's would reduce the uncertainty in the reactivity in general by $\sqrt{3}/3$ or around 58 %.

The detector signals needed for the IPEN/MB-01 reactivity meter with uncertainties came from the IPEN/MB-01 Data Acquisition System. This system collects all the operation data such as: control bank positions, temperatures, detector signals, reactivities, operation power, etc. and writes them in a computer file for further utilization. The operation data are also written in a rate of one set per second.

The IPEN/MB-01 reactivity meter with uncertainties could then be executed for each one of the three sets of kinetics parameters (CPSD, APSD1, and APSD2) employing the recovered detector signals from the Data Acquisition System files for the reactor operations considered here.

Table 9
Comparison between reactivity meter with uncertainties and IPEN(MB01)-LWR-RESR-15.

IPEN(MB01)-LWR-RESR-015					
	Reactivity Meter				IPEN(MB01)-LWR-RESR-015
	ρ(pcm)	σ_ρ^{corr}(pcm)	σ_ρ^{uncorr}(pcm)	$\rho \pm \sigma_\rho$(pcm)	$\rho \pm \sigma_\rho$(pcm)
Case 2–1 Nickel Plate					
CPSD	−339.46	19.21	0.69		
APSD1	−343.21	20.60	0.71		
APSD2	−343.48	16.56	0.81		
WeightedArithmeticMean	−342.15	10.71	0.81	−342.15 ± 10.74	−338.90 ± 12.29
Case 10–9 Nickel Plates					
CPSD	−175.06	7.82	0.73	–	–
APSD1	−177.36	8.37	0.74	–	–
APSD2	−176.98	6.68	1.03	–	–
Weighted Arithmetic Mean	−176.47	4.34	1.03	−176.47 ± 4.46	−173.49 ± 4.66
	Reactivity Meter				IPEN(MB01)-LWR-RESR-015
	$\Delta\rho^{(*)}$ (pcm)	σ_ρ^{corr}(pcm)	σ_ρ^{uncorr}(pcm)	$\Delta\rho \pm \sigma_\rho$(pcm)	$\Delta\rho \pm \sigma_\rho$(pcm)
Case 10 Reactivity Gain 9–8 Nickel Plates					
CPSD	50.03	0.31	0.19	–	–
APSD1	50.88	0.34	0.20	–	–
APSD2	50.27	0.26	0.28	–	–
Weighted Arithmetic Mean	50.36	0.17	0.28	50.36 ± 0.32	49.37 ± 0.17
Case 14 Reactivity Gain 18– 15 Nickel Plates					
CPSD	81.95	0.49	0.35	–	–
APSD1	83.39	0.52	0.36	–	–
APSD2	82.52	0.41	0.48	–	–
Weighted Arithmetic Mean	82.58	0.27	0.49	82.58 ± 0.56	81.80 ± 0.18

(*) Notation changed to be consistent to IPEN(MB01)-LWR-RESR-015.

Figure 4 shows the inferred reactivity data employing the IPEN/MB-01 reactivity meter with uncertainties for Case 10. Here, the results are shown only for the CPSD set of kinetics parameters and their correlated uncertainties. Also, the inferred reactivities are shown only for the time interval close to the plateau where the average reactivity was inferred. These inferred reactivities consist of the total reactivity inserted by the 9 Nickel plates relative to the case without Nickel plates (negative values in the figure) and the reactivity gain relative to Case 9 (positive values in the figure). These measurements arose from two different operations of the IPEN/MB-01 reactor. Figure 4 was built by merging the reactivity results of these two distinct operations. The time scale (y-axis) in Figure 4 is not the real time of the operation. The starting and end points of each reactor operation were chosen so that so that the main experimental data (the reactivity plateau region) were clearly shown. The data for Case 9 goes up to nearly 200 s while those for Case 10 goes beyond of that.

Similarly to the cases shown in Figures 1 and 2, it can be noted that the inferred reactivity as a function of time rapidly stabilizes. Figure 4 clearly shows the two plateaus relative to the reactivity gain ($\Delta\rho$) and the total reactivity (ρ). Contrary to that, the same did not occur for the uncertainty of the total reactivity for negative period. This reactivity uncertainty in the plateau time region increases up to a certain point and then stabilizes. The determination of the average reactivity and its uncertainty was carried out employing as before the average weighting average mean approach giving, respectively by Eqs. (46) for the reactivity and (48) for its uncertainty. The black bars shown in Figure 4 delimit the time interval for the weighting average mean application.

Table 9 shows the comparison of the reactivities, and their uncertainties reported in IPEN(MB01)-LWR-RESR-015 to those of the present paper. Here, the results of the reactivity meter with uncertainty are shown for all the spectral densities and for the correlated and uncorrelated and total uncertainties. The weighted arithmetic mean technique was employed for the determination of the reactivity meter average results for each spectral density similarly to that shown in Figure 4. The last line for each Case gives the weighted average values of all three spectral densities. Here the uncertainty of the final average reactivity follows the normal procedure of the weighted mean average. NF in Eq. (47) is replaced by 1. The three reactivity estimates (CPSD, APSD1, and APSD2) can be considered independent among them. Finally, the highest value of the uncorrelated uncertainty was considered in the determination of the total uncertainty.

Initially, Table 9 reveals that the reactivity meter inferred reactivities weakly depend on the type of the spectral density (CPSD, APSD1, APSD2). This is verified for all cases of Table 9. This is a good finding since it indicates that the delayed neutron data inferred from these spectral densities produce consistent results. Consequently, the IPEN (MB01)-LWR-RESR-015 hypotheses of using only the CPSD data for the determination of the average reactivity values can be considered justified. Further to that, The IPEN(MB01)-LWR-RESR-015 reactivities are inside of the 3-σ range of the reactivity meter uncertainties. This is clearly shown for Case 10. Also, the comparisons shown for Cases 2, and 10 indicates that the IPEN(MB01)-LWR-RESR-015 reactivity uncertainties are slightly overpredicted. The same does not occur for the reactivity gain cases. The uncertainty comparisons reveal that the approach adopted in the IPEN(MB01)-LWR-RESR-015 evaluation given by Eq (49) appears to cancel the uncorrelated part of the reactivity uncertainty. The reactivity gain for Case 10 shows this tendency. Case 14 has the highest reactivity gain and shows a high uncertainty discrepancy mostly due to its uncorrelated uncertainty part. This finding seems to be systematic for all positive reactivity gains.

5. Conclusion

The IPEN/MB-01 reactivity meter with uncertainties was successfully developed and implemented in this facility. This work shows that the model adopted for the reactivity uncertainty propagation was not only practical and feasible to be implemented but also its uncertainty results come into a very good agreement when compared to those originated from the Inhour Equation. The whole set of experimental kinetics parameters measured at the IPEN/MB-01 reactor and available to the international community through the NEA IRPhE project is of excellent quality, is unique in the reactor physics field and shows itself to be of extreme value to reduce the reactivity uncertainty values. The practical examples considering IPEN(MB01)-LWR-RESR-015 and the analyses preformed with the IPEN/MB-01 reactivity meter with uncertainties show that the uncertainties, respectively for negative and

positive reactivities is of the order of 3 % and 1 %. This is a good advance when compared to the results of previous work (dos Santos and Diniz, 2014) which reported uncertainties as high as 6 %. The uncertainty values employed in the IPEN/MB-01 reactivity meter have now a traceable route and although specific for the fuel rod core they can be of extreme help either to correct or to justify the uncertainty analyses made in several reactivity benchmarks performed in this facility.

Declaration of competing interest

The authors declare that they have no known competing financial interests or personal relationships that could have appeared to influence the work reported in this paper.

Data availability

Data will be made available on request.

References

Andersson, A.J.W., Hveding, T., 1964. A Reactivity Meter Design Used at HBWR. Report HPR-44.

ANSI, 1997. American National Standard for Expressing Uncertainty–U.S. Guide to the Expression of Uncertainty in Measurement. ANSI/NCSL Z540-2-1997.

Ball T.A., 2017. The Inverse Kinetics Method and Its Application to the Annular Core Research Reactor. https://digitalrepository.unm.edu/ne_etds/66.

Bell, G.I., Glasstone, S., 1979. Nuclear reactor theory. Van Nostrand Reinhold, New York.

Blaise, P., Mellier, F., Fougeras, P., 2009. Application of the modified source multiplication (MSM) technique to subcritical reactivity worth measurements in thermal and fast reactor systems. In: 1st International Conference on Advancements in Nuclear Instrumentation, Measurement Methods and Their Applications, pp. 1–9.

Brady, M.C., England, T.R., 1989. Delayed neutron data and group parameters for 43 fissioning systems. Nucl. Sci. Eng. 103 (2), 129–149.

Brown, D.A., Chadwick, M.B., Capote, R.A.C. Kahler, A. Trkov, M.W. Herman, A.A. Sonzogni, Y. Danon, A.D. Carlson, M. Dunn, D.L. Smith, G.M. Hale, G. Arbanas, R. Arcilla, C.R. Bates, B. Beck, B. Becker, F. Brown, R.J. Casperson, J. Conlin, D.E. Cullen, M.-A. Descalle, R. Firestone, T. Gaines, K.H. Guber, A.I. Hawari, J. Holmes, T. D. Johnson, T. Kawano, B.C. Kiedrowski, A.J. Koning, S. Kopecky, L. Leal, J.P. Lestone, C. Lubitz, Márquez Damián, J.I., Mattoon, C.M., McCutchan, E.A., Mughabghab, S., Navratil, P., Neudecker, D., Nobre, G.P.A., Noguere, G., Paris, M., Pigni, M. T., Plompen, A.J., Pritychenko, B., Pronyaev, V.G., Roubtsov, D., Rochman, D., Romano, P., Schillebeeckx, P., Simakov, S., Sin, M., Sirakov, I., Sleaford, B., Sobes, V., Soukhovitskii, E.S., Stetcu, I., Talou, P., Thompson, I., van der Marck, S., Welser-Sherrill, L., Wiarda, D., White, M., Wormald, J.L., Wright, R. Q., Zerkle, M., Žerovnik, G., Zhu, Y., 2018. ENDF/B-VIII.0: The 8th Major Release of the Nuclear Reaction Data Library with CIELO-project Cross Sections, New Standards and Thermal Scattering Data, Nuclear Data Sheets, 148, 1-142. ISSN 0090-3752.

Diniz, R., dos Santos, A., 2006. Experimental determination of the decay constants and abundances of delayed neutrons by means of reactor noise analysis. Nucl. Sci. Eng. 152 (2), 125–141.

dos Santos, A., 2021. IPEN(MB01)-LWR-RESR-021 benchmark of reactivity determination to support validation of evaluated delayed neutron data, international handbook of evaluated reactor physics benchmark experiments. Nuclear Energy Agency, Paris.

dos Santos, A., Diniz, R., 2020. The correlation matrix for the effective delayed neutron parameters of the IPEN/MB-01 reactor. Annals of Nuclear Energy, 136, 107008. ISSN 0306-4549.

dos Santos, A., Diniz, R., 2014. The evaluation of the effective kinetic parameters and reactivity of the IPEN/MB-01 reactor for the international reactor physics experiment evaluation project. Nucl. Sci. Eng. 178 (4), 459–478.

dos Santos, A., Diniz, R., Fanaro, L.C.C.B., Jerez, R., Andrade e Silva, G.S., Yamaguchi, M., 2006a. A proposal of a benchmark for β_{eff}, β_{eff}/Λ and Λ of thermal reactors fueled with slightly enriched uranium. Ann. Nucl. Energy 33 (9), 848–855.

dos Santos, A., Diniz, R., Jerez, R., Mai, L.A., Yamaguchi, M., 2006b. The application of the multiple transient technique for the experimental determination of the relative abundances and decay constants of delayed, neutrons of the IPEN/MB-01 reactor. Ann. Nucl. Energy 33 (10), 917–923.

dos Santos, A., Andrade e Silva, G.S., Fanaro, L. C.C.B., Yamaguchi, M., Jerez, R., Fuga, R., Mura, L.F.L., Abe, A.Y., 2014 IPEN(MB01)-LWR-RESR-015 Reactivity Effects of Nickel Reflector in the IPEN/MB-01 Research Reactor Facility. International Handbook of Evaluated Reactor Physics Benchmark Experiments. Paris: Nuclear Energy Agency.

dos Santos A., Andrade e Silva, G.S., Fanaro, L.C.C.B., Yamaguchi, M., Jerez, R., Diniz, R., Kuramoto, R.Y.R., 2012, IPEN(MB01)-LWR-001, Reactor Physics Experiments in the IPEN/MB-01 Research Reactor Facility. International Handbook of Evaluated Reactor Physics Benchmark Experiments. Paris: Nuclear Energy Agency, Paris (March Edition 2012).

Dulla, S., Nervo, M., Ravetto, P., 2014 A method for on-line reactivity monitoring in nuclear reactors. Annals of Nuclear Energy, 65, 433-440. ISSN 0306-4549.

Dulla, S., Hoh, S.S., Marana, G., Nervo, M., Ravetto, P., Pyeon, C.H., 2017. Analysis of KUCA measurements by the reactivity monitoring MAρTA method. Ann. Nucl. Energy 101, 397–407.

Fermi, E., 1946. The Development of the First Chain Reacting Pile. Proceedings of the American Philosophical Society, 90(1), Symposium on Atomic Energy and Its Implications, 20-24. Group Parameters. Progress in Nuclear Energy, 41(1-4), 145-201. LA-UR-98-918.

Hassan, Y.A., Chaplin, R.A., 2010. Nuclear energy materials and reactors-volume I. EOLSS Publications.

Henry, A.F., 1958. The application of reactor kinetics to the analysis of experiments. Nucl. Sci. Eng. 3 (1), 52–70.

Huo, X., Fan, Z., Xu, L., Chen, X., Hu, Y., Yu, H., 2019. A new and efficient method to measure reactivity in a nuclear reactor. Ann. Nucl. Energy 133, 455–457.

Keepin, G.R., Wimett, T.F., Zeigler, R.K., 1957. Delayed neutrons from fissionable isotopes of uranium. Plutonium and Thorium. Physical. Review 107 (4), 1044–1049.

Kinard, M. and Allen, E. J., 2004. Efficient numerical solution of the point kinetics equations in nuclear reactor dynamics. Annals of Nuclear Energy, 31(9), 1039-1051. ISSN 0306-4549.

Krása A., Kochetkov A, Messaoudi N, Vittiglio G, Wagemans J, 2021. The applicability range of the Modified Source Multiplication (MSM) method tested in the fast VENUS-F reactor. PHYSOR2020 – International Conference on Physics of Reactors: Transition toa Scalable Nuclear Future, Cambridge, UK. RPJ Web of Conferences, 247, 08001.

Kuramoto, R.Y.R., dos Santos, A., Jerez, R., Diniz, R., 2007. Absolute measurement of beff based on feynman-α experiments and the two-region model in the IPEN/MB-01 research reactor. Ann. Nucl. Energy 34 (6), 433–442.

Kuramoto, R.Y.R., dos Santos, A., Jerez, R., Diniz, R., 2008. Absolute measurement of beff based on rossi-a experiments and the two-region model in the IPEN/MB-01 research reactor. Nucl. Sci. Eng. 158 (3), 272–283.

Lee, E.K., Shin, H.C., Bae, S.M., Lee, Y.K., 2005. New dynamic method to measure rod worths in zero power physics test at PWR startup. Ann. Nucl. Energy 32 (13), 1457–1475.

MacFarlane, R. E., Muir, D. W., Boicourt, R. M., Kahler, A. C., Conlin, J. L., 2017. The NJOY Nuclear Data Processing System, Version 2016. Los Alamos National Laboratory, Los Alamos, USA. LA-UR—17-20093.

Marie, N., Lecouey, J.L., Lehaut, G., Chevret, T., Billebaud, A., Chabod, S., Doligez, X., Kochetkov, A., Krása, A., Lecolley, F.R., Mellier, F., Uyttenhove, W., Vittigli, G., Wagemans, J., 2019. Reactivity monitoring of the accelerator driven VENUS-F subcritical reactor with the “current-to-flux” method. Ann. Nucl. Energy 128, 12–23.

Momura, T., 1966. Reactivity measurements by reactor noise analysis using two-detector correlation method. J. Nucl. Sci. Technol. 3 (1), 14–19.

Muñoz-Cobo, J.L., Rugama, Y., Valentine, T.E., Mihalczo, J.T., Perez, R.B., 2001. Subcritical reactivity monitoring in accelerator driven systems. Ann. Nucl. Energy 28 (15), 1519–1547.

Ott, K.O., Neuhold, R.J., 1985. Introductory nuclear reactor dynamics. American Nuclear Society, La Grange Park, Illinois, USA.

Press, W.H., Teukolsky, S.A., Vetterling, W.T., Flannery, B.P., 1992. Numerical recipes in fortran, 2nd Edition. Cambridge University Press, Cambridge. Chapter 16.

Santos, D.F., dos Santos, A., 2021. Zero-power noise up to 100 kHz in the IPEN/MB-01 research reactor facility. Ann. Nucl. Energy 152, 107974.

Sastre, C.A., 1960. The measurement of reactivity. Nucl. Sci. Eng. 8, 433–447.

Shibata, K., Iwamoto, O., Nakagawa, T., Iwamoto, N., Ichirara, A., Kunieda, S., Chiba, S., Furutaka, K., Otuka, N., Ohsawa, T., Murata, T., Matsunobu, H., Zukeran, A., Kamada, S., Katakura, J., 2011. JENDL-4.0: a new library for nuclear science and engineering. J. Nucl. Sci. Technol. 48 (1), 1–30.

Spriggs, G.D., 1993. In-pile measurement of the decay constants and relative abundance of delayed neutrons. Nucl. Sci. Eng. 114 (4), 342–351.

Spriggs, G. D. and Campbell, J. M., 2000. A Summary of Measured Delayed Neutron.

Spriggs, G.D., Campbell, J.M., Piksaikin, V.M., 2002. An 8-group delayed neutron model based on a consistent set of half-lives. Prog. Nucl. Energy 41 (1–4), 223–251.

Suzuki, E., Tsunoda, T., 1964. A reactivity meter and its application. J. Nucl. Sci. Technol. 1 (6), 210–218.

Tamura, S., 2003. Signal fluctuation and neutron source in inverse kinetics method for reactivity measurement in the sub-critical domain. J. Nucl. Sci. Technol. 40 (3), 153–157.

Trkov, A., Herman, M., Brown, D. A., 2018. ENDF-6 Formats Manual: Data Formats and Procedures for the Evaluated Nuclear Data Files ENDF/B-VI, ENDF/B-VII and ENDF/B-VIII. CSEWG Document ENDF-102, Report BNL-203218-2018-INRE, SVN Commit: Revision 215.

Vo, VT., Nguyen, VK., Le, VD., Phan, QM., Phan, LS., Nguyen, HB., Nguyen, ND., 2023. A Digital Controller for Reactivity Monitoring and Power Control. Science and Technology of Nuclear Installations, 2023, 1-12. Article ID 2839654.

Wilson, W.B., England, T.R., 2002. Delayed neutron study using ENDF/B-VI basic nuclear data. Prog. Nucl. Energy 41 (1–4), 71–107. ISSN 0149–1970.

Zhang, N.F., 2006. The uncertainty associated with the weighted mean of measurement data. Metrologia 43 (3), 195–204.